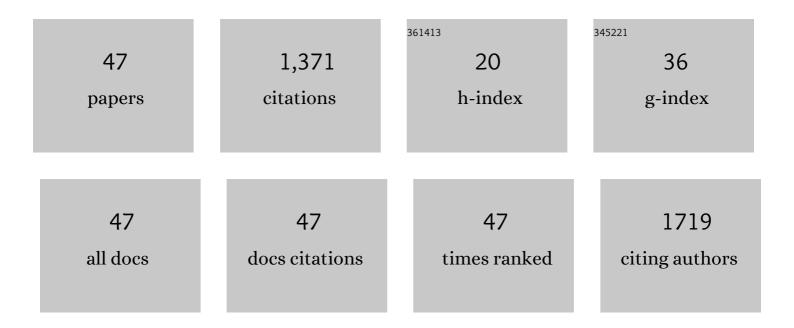
Lawrence Yao

List of Publications by Year in descending order

Source: https://exaly.com/author-pdf/11796985/publications.pdf Version: 2024-02-01



LAWDENCE YAO

#	Article	IF	CITATIONS
1	Sarcopenia in rheumatic disorders: what the radiologist and rheumatologist should know. Skeletal Radiology, 2022, 51, 513-524.	2.0	6
2	Preliminary validation of muscle ultrasound in juvenile dermatomyositis (JDM). Rheumatology, 2022, 61, SI48-SI55.	1.9	6
3	Vertebral Bone Mineral Density, Vertebral Strength, and Syndesmophyte Growth in Ankylosing Spondylitis: The Importance of Bridging. Arthritis and Rheumatology, 2022, 74, 1352-1362.	5.6	6
4	Sacroiliac Bone Marrow Edema: Innocent Until Proven Guilty?. Arthritis and Rheumatology, 2022, 74, 1474-1476.	5.6	1
5	Diagnosing sarcopenia at the point of imaging care: analysis of clinical, functional, and opportunistic CT metrics. Skeletal Radiology, 2021, 50, 543-550.	2.0	9
6	Janus kinase (JAK) inhibition with baricitinib in refractory juvenile dermatomyositis. Annals of the Rheumatic Diseases, 2021, 80, 406-408.	0.9	53
7	Rapidly progressive idiopathic arthritis of the hip: incidence and risk factors in a controlled cohort study of 1471 patients after intra-articular corticosteroid injection. Skeletal Radiology, 2021, 50, 2449-2457.	2.0	12
8	Subchondroplasty of the Ankle and Hindfoot for Treatment of Osteochondral Lesions and Stress Fractures: Initial Imaging Experience. Foot and Ankle Specialist, 2020, 13, 306-314.	1.0	6
9	Tears in the distal superficial medial collateral ligament: the wave sign and other associated MRI findings. Skeletal Radiology, 2020, 49, 747-756.	2.0	13
10	Use of Magnetic Resonance Imaging to Identify Immune Checkpoint Inhibitor–Induced Inflammatory Arthritis. JAMA Network Open, 2020, 3, e200032.	5.9	17
11	The Relationship of Static Tibial Tubercle–Trochlear Groove Measurement and Dynamic Patellar Tracking. American Journal of Sports Medicine, 2017, 45, 1856-1863.	4.2	26
12	Zygapophyseal Joint Fusion in Ankylosing Spondylitis Assessed by Computed Tomography: Associations with Syndesmophytes and Spinal Motion. Journal of Rheumatology, 2017, 44, 1004-1010.	2.0	22
13	The Tibial Tubercle–Trochlear Groove Distance Is Greater in Patients With Patellofemoral Pain: Implications for the Origin of Pain and Clinical Interventions. American Journal of Sports Medicine, 2017, 45, 1110-1116.	4.2	29
14	Thoracic Syndesmophytes Commonly Occur in the Absence of Lumbar Syndesmophytes in Ankylosing Spondylitis: A Computed Tomography Study. Journal of Rheumatology, 2017, 44, 1828-1832.	2.0	10
15	Magnetic resonance measurement of muscle T2, fat-corrected T2 and fat fraction in the assessment of idiopathic inflammatory myopathies. Rheumatology, 2016, 55, kev344.	1.9	41
16	Influence of IV Contrast Administration on CT Measures of Muscle and Bone Attenuation: Implications for Sarcopenia and Osteoporosis Evaluation. American Journal of Roentgenology, 2016, 207, 1046-1054.	2.2	57
17	Spatial distribution of syndesmophytes along the vertebral rim in ankylosing spondylitis: preferential involvement of the posterolateral rim. Annals of the Rheumatic Diseases, 2016, 75, 1951-1957.	0.9	17
18	Quantitative syndesmophyte measurement in ankylosing spondylitis using CT: longitudinal validity and sensitivity to change over 2 years. Annals of the Rheumatic Diseases, 2015, 74, 437-443.	0.9	31

LAWRENCE YAO

#	Article	IF	CITATIONS
19	Imatinib Mesylate for the Treatment of Steroid-Refractory Sclerotic-Type Cutaneous Chronic Graft-versus-Host Disease. Biology of Blood and Marrow Transplantation, 2015, 21, 1083-1090.	2.0	53
20	The Notch of Harty (Pseudodefect of the Tibial Plafond): Frequency and Characteristic Findings at MRI of the Ankle. American Journal of Roentgenology, 2015, 205, 358-363.	2.2	7
21	Sarcopenia: Current Concepts and Imaging Implications. American Journal of Roentgenology, 2015, 205, W255-W266.	2.2	232
22	Quantitation of Circumferential Syndesmophyte Height along the Vertebral Rim in Ankylosing Spondylitis Using Computed Tomography. Journal of Rheumatology, 2015, 42, 472-478.	2.0	9
23	Dynamics of syndesmophyte growth in AS as measured by quantitative CT: heterogeneity within and among vertebral disc spaces. Rheumatology, 2015, 54, 972-980.	1.9	7
24	Quantitative measurement of syndesmophyte volume and height in ankylosing spondylitis using CT. Annals of the Rheumatic Diseases, 2014, 73, 544-550.	0.9	31
25	Axial Scan Orientation and the Tibial Tubercle–Trochlear Groove Distance: Error Analysis and Correction. American Journal of Roentgenology, 2014, 202, 1291-1296.	2.2	34
26	Quantitative Monitoring of Syndesmophyte Growth in Ankylosing Spondylitis Using Computed Tomography. Lecture Notes in Computational Vision and Biomechanics, 2014, , 135-142.	0.5	0
27	High precision semiautomated computed tomography measurement of lumbar disk and vertebral heights. Medical Physics, 2013, 40, 011905.	3.0	8
28	Improved precision of syndesmophyte measurement for the evaluation of ankylosing spondylitis using CT: a phantom and patient study. Physics in Medicine and Biology, 2012, 57, 4683-4704.	3.0	12
29	High precision semi-automated vertebral height measurement using computed tomography: A phantom study. , 2012, 2012, 1554-7.		2
30	Fat-Corrected T2 Measurement as a Marker of Active Muscle Disease in Inflammatory Myopathy. American Journal of Roentgenology, 2012, 198, W475-W481.	2.2	49
31	Diagnosis, management, and complications of glomus tumours of the digits in neurofibromatosis type 1. Journal of Medical Genetics, 2010, 47, 525-532.	3.2	61
32	Precision of syndesmophyte volume measurement for ankylosing spondylitis: A phantom study using high resolution CT. , 2009, 2009, 3577-80.		0
33	Glomus Tumors in Neurofibromatosis Type 1: Genetic, Functional, and Clinical Evidence of a Novel Association. Cancer Research, 2009, 69, 7393-7401.	0.9	122
34	Magnetic Resonance Imaging in Sclerotic-Type Chronic Graft-vs-Host Disease. Archives of Dermatology, 2009, 145, 918-22.	1.4	18
35	Computer Aided Evaluation of Ankylosing Spondylitis Using High-Resolution CT. IEEE Transactions on Medical Imaging, 2008, 27, 1252-1267.	8.9	33
36	Vertebral surface registration using ridgelines/crestlines. Proceedings of SPIE, 2008, , .	0.8	4

LAWRENCE YAO

#	Article	IF	CITATIONS
37	3D Multi-scale level set segmentation of vertebrae. , 2007, , .		7
38	Isotropic 3D Fast Spin-Echo with Proton-Density-Like Contrast: A Comprehensive Approach to Musculoskeletal MRI. American Journal of Roentgenology, 2007, 188, W199-W201.	2.2	36
39	Periarticular Bone Findings in Rheumatoid Arthritis: T2-Weighted Versus Contrast-Enhanced T1-Weighted MRI. American Journal of Roentgenology, 2006, 187, 358-363.	2.2	13
40	Presumptive subarticular stress reactions of the knee: MRI detection and association with meniscal tear patterns. Skeletal Radiology, 2004, 33, 260-264.	2.0	79
41	Infraspinatus Muscle Atrophy: Implications?. Radiology, 2003, 226, 161-164.	7.3	33
42	Magnetization Transfer Contrast in Rapid Three-Dimensional MR Imaging Using Segmented Radiofrequency Prepulses. American Journal of Roentgenology, 2002, 179, 863-865.	2.2	0
43	Saline versus gadolinium-enhanced magnetic resonance arthrography of porcine cartilage. Academic Radiology, 1997, 4, 127-131.	2.5	6
44	Incidental magnetization transfer contrast in fast spin-echo imaging of cartilage. Journal of Magnetic Resonance Imaging, 1996, 6, 180-184.	3.4	73
45	MR imaging of tibial collateral ligament injury: comparison with clinical examination. Skeletal Radiology, 1994, 23, 521-4.	2.0	45
46	Magnetic Resonance Imaging of Osseous Lesions of the Knee. Physician and Sportsmedicine, 1990, 18, 81-84.	2.1	4
47	Occult intraosseous fracture: Magnetic resonance appearance versus age of injury. American Journal of Sports Medicine, 1989, 17, 620-623	4.2	31